Journal of Advanced Ceramics

Volume 3 | Issue 3 Article 7

2014

Role of phonon drag and carrier diffusion in thermoelectric power of polycrystalline $La_{0.97}Na_{0.03}MnO_3$ manganites

Dinesh VARSHNEY
Materials Science Laboratory, School of Physics, Vigyan Bhawan, Devi Ahilya University, Khandwa Road Campus, Indore 452001, India

Dinesh CHOUDHARY
Materials Science Laboratory, School of Physics, Vigyan Bhawan, Devi Ahilya University, Khandwa Road Campus, Indore 452001, India

Recommended Citation

Dinesh VARSHNEY, Dinesh CHOUDHARY. Role of phonon drag and carrier diffusion in thermoelectric power of polycrystalline La0.97Na0.03MnO3 manganites. Journal of Advanced Ceramics 2014, 3(3): 224-229.

Journal of Advanced Ceramics
2014, 3(3): 224–229
DOI: 10.1007/s40145-014-0113-1

ISSN 2226-4108
CN 10-1154/TQ

Research Article

Role of phonon drag and carrier diffusion in thermoelectric power of polycrystalline $La_{0.97}Na_{0.03}MnO_3$ manganites

Dinesh VARSHNEY*, Dinesh CHOUDHARY

Materials Science Laboratory, *School of Physics*, *Vigyan Bhawan*, *Devi Ahilya University*, *Khandwa Road Campus*, *Indore 452001*, *India*

Received: April 04, 2014; Revised: June 09, 2014; Accepted: June 14, 2014

Abstract: We develop a theoretical model for quantitative analysis of temperature-dependent thermoelectric power of monovalent (Na) doped $La_{0.97}Na_{0.03}MnO_3$ manganites. In the ferromagnetic regime, we have evaluated the phonon thermoelectric power by incorporating the scattering of phonons with impurities, grain boundaries, charge carriers and phonons. In doing so, we use the Mott expression to compute the carrier (hole) diffusion thermoelectric power (S_c^{diff}) using Fermi energy as carrier (hole)-free parameter, and S_c^{diff} shows linear temperature dependence and phonon drag S_{ph}^{drag} increases exponentially with temperature which is an artifact of various operating scattering mechanisms. It is also shown that for phonons the scattering and transport cross-sections are proportional to ω^4 in the Rayleigh regime where ω is the frequency of the phonons. Numerical analysis of thermoelectric power from the present model shows similar results as those revealed from experiments.

Keywords: phonon drag; carrier diffusion; thermoelectric power

1 Introduction

The mixed-valence perovskite manganites $Ln_{1-x}A_xMnO_3$ (with Ln = La, Pr, Nd, Eu, etc., and A = Ca, Sr, Ba, Na, K, Ag, etc.) have recently attracted considerable attention because of a huge negative magnetoresistance (colossal magnetoresistance, CMR) near the Curie temperature [1]. A number of works has recently been devoted to studying the interplay among structure, magnetism and transport in manganese perovskites. This behavior has been interpreted on the basis of the double-exchange (DE) theory [2] and the dynamic Jahn–Teller (J–T) effect [3]. Thorough investigation has been made showing evidence in favor of strong carrier (hole)–phonon coupling due to J–T ions, which has also been considered to play a key role in transport mechanism of these manganites [4].

$Ln_{1-x}A_xMnO_3$ compounds have been studied most extensively. It is of interest to substitute alkali-metal ions for La because the large difference in valence may lead to changes in structure and magnetic properties. It is known that the host atom La and the doped atom Na have approximately equal ionic radius ($R_{La^{3+}} = 1.36$ Å, $R_{Na^+} = 1.39$ Å) [5]. Switching from divalent to the monovalent doping (A = Na or K) in $Ln_{1-x}A_xMnO_3$, since the valence state of sodium is +1, for every sodium ion substitution for trivalent lanthanum ion, two Mn^{3+} need to be oxidised to Mn^{4+} and hence the cation valency distribution can be represented as $La^{3+}_{1-x}Na^+_x(Mn^{3+}_{1-2x}Mn^{4+}_{2x})O_3$ [6].

Thermoelectric power $S(T)$ is known to be very sensitive even to the slightest variations in the magnetic and electrical properties, which are not easily

* Corresponding author.
E-mail: vdinesh33@rediffmail.com

observable in magnetization and resistivity studies. Various properties of materials, such as sign of the charge carriers, carrier concentration and magnetic and electronic phase transitions, etc., can be understood by studying $S(T)$ [7]. Further, thermopower studies also help to understand the influence of some contributing factors of $S(T)$ including diffusion, magnon drag, phonon drag and spin fluctuations along with their relative weights. Therefore, it is strongly believed that $S(T)$ is technically important and scientifically interesting to investigate various types of solids in general and manganites in particular [8].

The change in sign in the $S(T)$ data of the samples indicates the coexistence of two types of carriers. The negative S at high temperature is attributed to the electrons as carriers which are excited from the valence band into the conduction band. Because of the higher mobility of electrons within the conduction band, S is negative. At low temperature, the electrons in the valence band are excited into the impurity band which generates hole-like carriers, which is responsible for a positive S. Keeping all these facts in mind, a systematic study of influence of monovalent Na doping in parent $LaMnO_3$ on thermopower of $La_{0.97}Na_{0.03}MnO_3$ has been carried out and the results of such an investigation are presented here.

The paper is structured as follows. In Section 2, we give details about the scattering rates within the relaxation time approximation to estimate the phonon drag contribution towards $S(T)$, incorporating the scattering of phonons with defects, holes as carriers, grain boundaries and phonon–phonon interactions, respectively. Later on, the role of carrier diffusion contribution towards $S(T)$ is investigated. In Section 3, we give the numerical estimation of various scattering rates for the calculation of diffusion and phonon drag processes and discuss the results obtained. The final part of the paper is devoted to conclusions and is presented in Section 4.

2 Model

We follow a simple model where the phonons are described in the Debye model and the hopping of charge carriers is treated in an isotropic double exchange model. The use of the Debye model is reasonable in manganites and cuprates since the temperature region of interest lies well below the Debye temperature [9–14]. As the simplest approximation to the problem at hand, the isotropic Debye model approach is used to derive qualitative results, as we will demonstrate later. We start with a model Hamiltonian that follows [9]

$$\begin{aligned} H = & \sum_k \varepsilon_k a_k^+ a_k + \sum_q \omega_q b_q^+ b_q + \sum_{k_1,k_2} \phi(k_1,k_2) a_{k_1}^+ a_{k_2} \\ & + D_\mathrm{p} \sum_{k,q} q \left(\frac{\hbar}{2\rho\omega_q} \right)^{1/2} a_{k+q}^+ a_k (b_k + b_{-k}^+) \\ & + \frac{R}{2N} \sum_{q_1,q_2} \mathrm{e}^{\mathrm{i}(q_1+q_2)r_i} \left(\frac{\hbar\omega_{q_1} \hbar\omega_{q_2}}{4} \right)^{1/2} (b_{q_1} - b_{-q_1}^+)(b_{q_2} - b_{-q_2}^+) \\ & + H_{\mathrm{ph-ph}} \end{aligned} \tag{1}$$

Here, the initial two terms are carriers and phonon excitations. The third and fourth terms represent the carrier–impurity interactions and carrier–phonon interactions, respectively. The fifth and sixth terms denote the phonon–impurity and the phonon–phonon interactions, respectively.

The notations a^+ (a) and b^+ (b) are the creation (annihilation) operators for carriers and phonons, respectively. D_p is the deformation-potential constant, and R is the relative ionic-mass difference $(M'' - M)/M''$. The phonon frequency of a wave vector q is ω_q. N is the number of cells. ρ is the mass density of ions, and r_i stands for the position of defects. ε_k is the hole free energy.

The thermopower following model Hamiltonian (Eq. (1)) can be calculated from the Kubo formula [15]. It has contributions from both phonons and carriers. We first explore the lattice part. In the continuum approximation [16]

$$S_\mathrm{ph}^\mathrm{drag}(T) = -\frac{k_\mathrm{B}}{|e|} \left(\frac{T}{\theta_\mathrm{D}} \right)^3 \int_0^{\omega_\mathrm{D}} \mathrm{d}\omega (\beta\omega)^4 A(\omega) \frac{\mathrm{e}^{\beta\omega}}{(\mathrm{e}^{\beta\omega} - 1)^2} \tag{2}$$

where k_B is the Boltzman constant; e is the charge of carriers; ω_D is the Debye frequency; and $\beta = \hbar / (k_\mathrm{B} T)$. The relaxation time is inhibited in $A(\omega)$ and is proportional to the imaginary part of the phonon self-energy.

The phonon drag thermoelectric power relaxation time $A(\omega)$ is written as

$$\begin{aligned} A(\omega) = & (1/\tau_{\mathrm{ph-d}} + 1/\tau_{\mathrm{ph-gb}} + 1/\tau_{\mathrm{ph-ph}})^{-1} \\ & \times (1/\tau_{\mathrm{ph-d}} + 1/\tau_{\mathrm{ph-gb}} + 1/\tau_{\mathrm{ph-ph}} + 1/\tau_{\mathrm{ph-c}}) \end{aligned} \tag{3}$$

In the weak interaction case, it has been calculated to the lowest order of the various interactions. The relaxation time is expressed as

$$1/\tau(\omega) = 2|\mathrm{Im}\,P(\omega/v_s, \omega)| \quad (4)$$

The various relaxation time is defined in terms of transport coefficients as

$$\tau_{\mathrm{ph-d}}^{-1}(\omega) = D_{\mathrm{phd}}(\hbar/k_B)^3\omega^4 \quad (5)$$

$$\tau_{\mathrm{ph-gb}}^{-1}(\omega) = D_{\mathrm{phgb}}v_s/L \quad (6)$$

$$\tau_{\mathrm{ph-ph}}^{-1}(\omega) = D_{\mathrm{phph}}(T\omega\hbar/k_B)^3 \quad (7)$$

and

$$\tau_{\mathrm{ph-c}}^{-1}(\omega) = D_{\mathrm{phc}}\omega n_F \quad (8)$$

where L is the crystal dimension; n_F is the Fermi–Dirac distribution function. The notation $\tau_{\mathrm{ph-d}}$, $\tau_{\mathrm{ph-gb}}$, $\tau_{\mathrm{ph-ph}}$ and $\tau_{\mathrm{ph-c}}$ are the phonon scattering relaxation time due to defects, grain boundaries, and phonon and phonon–carrier interactions, respectively. It is worth to mention that this order Mathiessen's rule holds namely, that the inverse of the total relaxation time is the sum of the various contributions for the different scattering channels.

The transport coefficients appearing in Eqs. (5)–(8) are defined as

$$D_{\mathrm{phd}} = \frac{3n_i R^2}{4\theta_D^3} \quad (9)$$

and

$$D_{\mathrm{phc}} = \frac{9\pi}{4}\left(\frac{m}{3M}\right)^{1/2}\frac{D_p^2}{\varepsilon_F^2} \quad (10)$$

characterizing the strengths of the phonon–defect and phonon–hole scattering processes. Here, n_i is the density of impurities or defects, ε_F is the Fermi energy of holes as carriers and m is its mass.

Let us now proceed to include the effect of free carrier (hole) diffusion contribution towards thermoelectric power employing the well-known Mott formula. The low temperature carrier diffusion thermoelectric power is [17]

$$S_c^{\mathrm{diff}}(T) = -\frac{\pi^2 k_B^2 T}{3|e|}\left[\frac{\partial \ln\sigma(\varepsilon)}{\partial\varepsilon}\right]_{\varepsilon=\varepsilon_F} \quad (11)$$

where $\sigma(\varepsilon)$ $(=Ne^2\tau(\varepsilon_F)/m)$ is the energy dependence of conductivity in the relaxation time approximation. In what follows, the mean free path of the carriers (ℓ) is assumed to be independent of temperature. Equation (11) becomes

$$S_c^{\mathrm{diff}}(T) = -\frac{\pi^2 k_B^2 T}{3|e|\varepsilon_F} \quad (12)$$

with constant mean free path, and the method point to the scattering of carrier (hole) by impurities is dominant. We must point out that the linear response transport theory based on Fermi liquid description results in an exact expression for the most singular term in terms of damping rate and is valid for correlated electron systems as manganites. It is known that the third law of thermodynamics reveals that at zero temperature the heat capacity and thermoelectric power of metals are zero as quasiparticle relaxation time is finite due to defect scatterings. The estimation and numerical computation of the phonon drag and carrier (hole) diffusion contributions to the thermoelectric power by incorporating the effects of different scattering mechanisms are presented in the following section.

3 Results and discussion

For the analysis of the transport properties, it is essential to know realistic values of some physical parameters governing the thermoelectric power behavior. To gain additional insight into the mechanism responsible for the transport, we have carried out thermoelectric power studies with particular emphasis on carrier (hole) and phonon drag contributions for $S(T)$ in manganites. Using Hafemeister and Flygare type potential we find the force constant, κ, accounting for long-range Coulomb–van der Waals (vdW) interaction and the short-range repulsive interaction up to second neighbour ions as 1.096×10^4 g·m·s^{-2} for $La_{0.97}Na_{0.03}MnO_3$. With these parameters, the Debye temperature is estimated 561 K. Details of the method of calculation of characteristic frequencies and their relevant expressions are reported elsewhere [18–22]. The deduced value of the Debye temperature is consistent with the previously reported value (θ_D= 552 K for x = 0.05) for $La_{1-x}Na_xMnO_3$ manganites [23]. It is worth to mention that θ_D is a function of temperature and varies from technique to technique, and its value also varies from sample to sample with standard deviation of ±15 K.

While estimating the temperature-dependent thermoelectric power at low temperature of these samples, we make use of the transport parameters which characterize the strengths of the phonon–defect ($D_{\mathrm{ph-d}}=2\times10^{-13}$ K^{-3}), phonon–grain boundary ($D_{\mathrm{ph-gb}}=1.3\times10^{-8}$), phonon–phonon ($D_{\mathrm{ph-ph}}=9\times10^{-17}$ K^{-6}·s^{-1})

and phonon–carrier ($D_{\mathrm{ph-c}} = 1.9\times10^{-3}$) scattering processes. These are indeed material-dependent parameters for phonon drag thermoelectric power in the present model. In these calculations we used the length of sample of about 3 mm and $v_s = 3\times10^5$ cm·s^{-1}.

Let us first discuss the relative magnitudes of the various scattering mechanisms. Plots of various scattering phonon relaxation time as a function of ξ ($=\hbar\omega/(k_BT)$) in terms of frequency at $T = 50$ K and $T = 250$ K are shown in Fig. 1 for $La_{0.97}Na_{0.03}MnO_3$. It can be seen that for low value of ξ, the phonon–carrier (hole) scattering is higher, while for high value of ξ, it is the phonon–defect scattering that grows faster. On the other hand, at both small and large value of ξ, phonon–phonon scattering process is weaker at low temperature ($T = 50$ K) for both the samples. As we go with increase in temperature ($T = 250$ K) where phonons are excited in large numbers, phonon–phonon scattering dominates over phonon–defect scattering for low value of ξ.

We now qualitatively discuss the phonon drag thermoelectric power ($S_{\mathrm{ph}}^{\mathrm{drag}}$) in the presence of various scattering mechanisms (Fig. 2). At low temperature, the quasi particle excitations are condensed into the ground state and they cannot scatter phonons. $S_{\mathrm{ph}}^{\mathrm{drag}}$ thus increases exponentially with temperature in the low-temperature regime. In Fig. 2, we further compare the effect of various operating scatterings on thermopower. Initially when only phonon–grain boundaries (ph–gb) scattering is available,

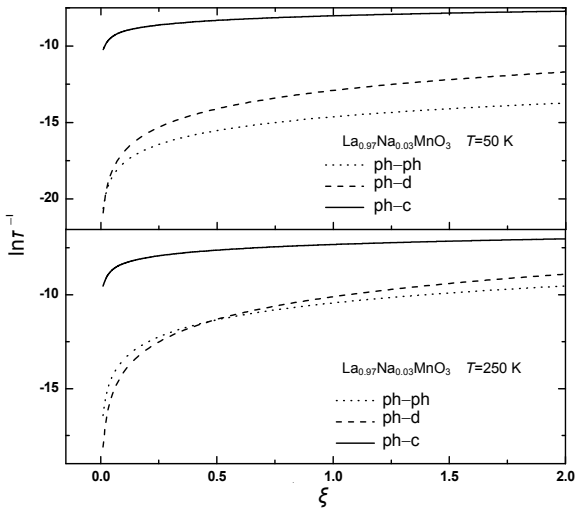

Fig. 1 Various phonon relaxation time as a function of $\xi=\hbar\omega/(k_BT)$ for $T = 50$ K and $T = 250$ K.

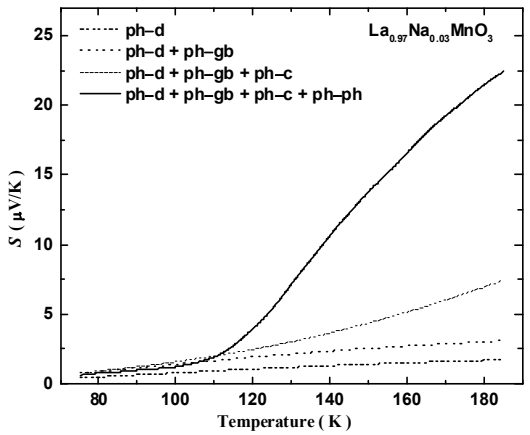

Fig. 2 Variations of phonon drag thermoelectric power as a function of temperature in presence of various phonon scattering mechanisms for $La_{0.97}Na_{0.03}MnO_3$.

thermoelectric power is minimum. As phonon–defect (ph–d) and phonon–carrier (hole) (ph–c) scatterings are included, they improve the thermopower. Further, when phonon–phonon (ph–ph) scattering is also included, since phonons are more active at higher temperature, it increases the thermopower mainly at higher temperature. The results show that the effect of scatterings on thermoelectric power is additive and the final variation depends on the relative magnitude of different scattering processes available. It is worth to mention that S is zero ($T\to0$ K) and that every non-zero value is an artifact due to the model. The scattering and transport cross-sections for phonons are proportional to ω^4 in the Rayleigh regime where ω is the frequency of phonons, which is also evidenced by the model Hamiltonian (Eq. (2)).

Let us now estimate the carrier (hole) diffusion thermoelectric power ($S_{\mathrm{c}}^{\mathrm{diff}}$) given by Eqs. (11) and (12), which is inversely proportional to Fermi energy. The carrier–impurity contribution to the thermoelectric power $S_{\mathrm{c}}^{\mathrm{diff}}$ is documented in Fig. 3 as a function of temperature. It is evident from the plot that $S_{\mathrm{c}}^{\mathrm{diff}}$ increases linearly with increasing temperature. Finally, both contributions are added together and plotted with the experimental data [24] in the same figure. Numerical analysis of thermoelectric power from the present model shows similar result as those revealed from experiments. $S(T)$ behavior depends on the competition among the various scattering mechanisms for the heat carriers and balances between the carrier (hole) and phonon competition.

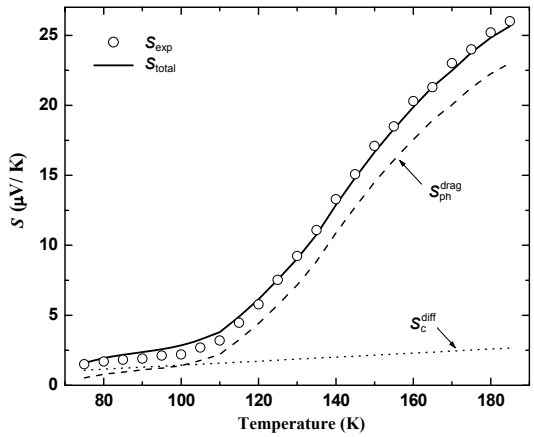

Fig. 3 Thermopower versus temperature along with experimental data for $La_{0.97}Na_{0.03}MnO_3$.

The importance of the present computation is in line with field of phononics that is aimed at manipulating the heat flow or related thermoelectric phenomena and information processing with phonons similar to that of electrons and photons. Enhancement of temperature infers substantial phonon–phonon scattering when a comparison has been made with phonon–defect and phonon–carrier. Within the framework of phonons, the effective phonon scattering mechanism for heat transport in manganites shall be helpful for the design of novel phononic devices [25].

4 Conclusions

The thermoelectric power $S(T)$ behavior is an instructive probe to reveal the phonon effects and carrier diffusion as well as the interaction of these excitations with one another, with impurities, grain boundaries and defects. Among various transport probes, it brings information about available subsystems and the measurements are fairly simple. The present study intends to contribute towards a thorough understanding of the scattering processes taking place in these fascinating manganites. This anomalous behavior is well explained by considering two channels for $S(T)$: carrier (hole) diffusion (S_c^{diff}) and phonon drag (S_{ph}^{drag}) and the competition among various scattering mechanisms.

The phonon drag (S_{ph}^{drag}) is discussed within the Debye-type relaxation rate approximation in terms of the acoustic phonon frequency, a relaxation time τ and the sound velocity. The rapid increase in $S(T)$ is attributed to increase in phonon mean free path due to carrier condensation in the low temperature domain limited by various impurity scattering mechanisms. The physical entities in the present scheme that characterize the strengths of the phonon–defect, phonon–hole, and phonon–phonon scatterings lead to a result that successfully retrace the experimental curve. The behavior of $S(T)$ is determined by competition among the several operating scattering mechanisms for the heat carriers and a balance between carrier (hole) diffusion and phonon drag contributions in the polycrystalline $La_{0.97}Na_{0.03}MnO_3$ manganites.

References

[1] Salamon MB, Jaime M. The physics of manganites: Structure and transport. *Rev Mod Phys* 2001, **73**: 583–626.

[2] De Gennes P-G. Effects of double exchange in magnetic crystals. *Phys Rev* 1960, **118**: 141–154.

[3] Millis AJ, Littlewood PB, Shraiman BI. Double exchange alone does not explain the resistivity of $La_{1-x}Sr_xMnO_3$. *Phys Rev Lett* 1995, **74**: 5144–5147.

[4] Jaime M, Lin P, Salamon MB, *et al.* Low-temperature electrical transport and double exchange in $La_{0.67}(Pb,Ca)_{0.33}MnO_3$. *Phys Rev B* 1998, **58**: R5901–R5904.

[5] Shannon RD. Revised effective ionic radii and systematic studies of interatomic distances in halides and chalcogenides. *Acta Cryst* 1976, **A32**: 751–767.

[6] Malavasi L, Mozzati MC, Ghigna P, *et al.* Lattice disorder, electric properties, and magnetic behavior of $La_{1-x}Na_xMnO_{3+\delta}$ manganites. *J Phys Chem B* 2003, **107**: 2500–2505.

[7] Mandal P. Temperature and doping dependence of the thermopower in $LaMnO_3$. *Phys Rev B* 2000, **61**: 14675–14680.

[8] Jaime M, Salamon MB, Rubinstein M, *et al.* High-temperature thermopower in $La_{2/3}Ca_{1/3}MnO_3$ films: Evidence for polaronic transport. *Phys Rev B* 1996, **54**: 11914–11917.

[9] Varshney D, Choudhary KK, Singh RK. Analysis of in-plane thermal conductivity anomalies in

$YBa_2Cu_3O_{7-\delta}$ cuprate superconductors. *New J Phys* 2003, **5**: 72.1–72.17.

[10] Varshney D, Kaurav N. Numerical analysis of heat transport behavior in the ferromagnetic metallic state of $La_{0.80}Ca_{0.20}MnO_3$ manganites. *J Low Temp Phys* 2007, **147**: 7–30.

[11] Varshney D, Kaurav N. Analysis of low temperature specific heat in the ferromagnetic state of the Ca-doped manganites. *Eur Phys J B* 2004, **37**: 301–309.

[12] Varshney D, Kaurav N. Low temperature specific heat analysis of $LaMnO_{3+\delta}$ manganites. *Int J Mod Phys B* 2006, **20**: 4785–4797.

[13] Varshney D, Singh RK, Khaskalam AK. Analysis of specific heat in $YBa_2Cu_3O_{7-\delta}$ ceramic superconductors. *Phys Status Solidi b* 1998, **206**: 749–757.

[14] Varshney D, Shah S, Singh RK. Specific heat studies in Ho–Ba–CuO superconductors: Fermionic and bosonic contributions. *Bull Mater Sci* 2000, **23**: 267–272.

[15] Callaway J. *Quantum Theory of the Solid State*. London: Academic Press, 1991.

[16] Barnard RD. *Thermoelectricity in Metals and Alloys*. London: Taylor and Francis Ltd., 1972.

[17] Mott NF, Davis EA. *Electronic Processes in Non-Crystalline Materials*. Oxford: Clarendon, 1979.

[18] Varshney D, Choudhary D, Shaikh MW. Interpretation of metallic and semiconducting temperature-dependent resistivity of $La_{1-x}Na_xMnO_3$ ($x = 0.07$, 0.13) manganites. *Comput Mater Sci* 2010, **47**: 839–847.

[19] Varshney D, Choudhary D, Shaikh MW, *et al*. Electrical resistivity behaviour of sodium substituted manganites: Electron–phonon, electron–electron and electron–magnon interactions. *Eur Phys J B* 2010, **76**: 327–338.

[20] Shaikh MW, Varshney D. Structural properties and electrical resistivity behaviour of $La_{1-x}K_xMnO_3$ ($x = 0.1$, 0.125 and 0.15) manganites. *Mater Chem Phys* 2012, **134**: 886–898.

[21] Varshney D, Dodiya N. Electrical resistivity of the hole doped $La_{0.8}Sr_{0.2}MnO_3$ manganites: Role of electron–electron/phonon/magnon interactions. *Mater Chem Phys* 2011, **129**: 896–904.

[22] Varshney D, Dodiya N. Interpretation of metallic and semiconducting temperature dependent resistivity of $La_{0.91}Rb_{0.06}Mn_{0.94}O_3$ manganites. *Solid State Sci* 2011, **13**: 1623–1632.

[23] Das S, Dey TK. Structural and magnetocaloric properties of $La_{1-y}Na_yMnO_3$ compounds prepared by microwave processing. *J Phys D*: *Appl Phys* 2007, **40**: 1855–1863.

[24] Vergara J, Ortega-Hertogs RJ, Madurga V, *et al*. Effect of disorder produced by cationic vacancies at the *B* sites on the electronic properties of mixed valence manganites. *Phys Rev B* 1999, **60**: 1127–1135.

[25] Dubi Y, Di Ventra M. Colloquium: Heat flow and thermoelectricity in atomic and molecular junctions. *Rev Mod Phys* 2011, **83**: 131.